Measurement of the physico-chemical properties of four pharmaceutical aerosols as they travel from pressurised metered dose inhalers (pMDI) to a model lung

N. Davidson[a#], H. -J. Tong[b#], M. Kalberer[b], P. C. Seville[c,d], A. D. Ward[e], M. K. Kuimova[f] and F. D. Pope[a*]

[a]School of Geography, Earth and Environmental Sciences, University of Birmingham, Edgbaston, Birmingham, B15 2TT, UK.

[b]Department of Chemistry, University of Cambridge, Lensfield Road, Cambridge, CB2 1EW, UK.

[c]School of Pharmacy, University of Birmingham, Edgbaston, Birmingham, B15 2TT, UK.

[d]School of Pharmacy and Biomedical Sciences, University of Central Lancashire, Preston, Lancs, PR1 2HE, UK.

[e]Central Laser Facility, Rutherford Appleton Laboratory, Harwell, Oxford, OX11 0QX, UK.

[f]Imperial College London, South Kensington Campus, London, SW7 2AZ, UK

[#]Both authors contributed equally to this paper

[*]Corresponding author
Dr Francis Pope
School of Geography, Earth and Environmental Sciences, University of Birmingham, Edgbaston, Birmingham, B15 2TT, UK.
f.pope@bham.ac.uk
Telephone – (+44) 0121 4149067

Key Words

Salbutamol sulfate, salmeterol xinafoate, fluticasone propionate, ciclesonide, desisobutyryl-ciclesonide, hygroscopicity, optical trapping, laser tweezers, suspended particle, pMDI

Abstract

Conditions of relative humidity and temperature inside the lungs are generally very different from the outside air, with the lung environment typically being warmer and of higher humidity. The change in temperature and humidity as pharmaceutical drugs pass from inhaler to lung environment can cause hygroscopic phase transitions and particle growth. This implies that inhalable drugs that do not exhibit hygroscopic properties under standard laboratory testing may behave differently inside the human body. To better examine these properties, solid particles injected directly from four different pressurised metered dose inhalers were stably captured in an optical trap and examined online via Raman spectroscopy. Micron-sized particles of salmeterol xinafoate, fluticasone propionate and ciclesonide were suspended and examined at a range of relative humidity conditions inside a chamber designed to mimic conditions inside the respiratory tract and lung. Particles of salbutamol sulfate were also examined under different temperature and relative humidity conditions to explore the effect of temperature upon their hygroscopicity. This technique allows inhalable drugs with hygroscopic properties to be tested to ensure that they are still within the optimum size range for retention within the lungs post inhalation.

1. Introduction

1.1 Respiratory drugs and drug delivery

Respiratory ailments in the form of asthma and Chronic Obstructive Pulmonary Disease (COPD) are managed with inhalable drugs. These drugs include beta-2 agonists such as salbutamol and salmeterol, and corticosteroids like fluticasone and ciclesonide.

Salbutamol sulfate and salmeterol xinafoate are both *beta-2 andrenoceptor agonists*, meaning that they target the beta-2 receptors in bronchial muscle cells in a similar manner to adrenaline (Reisine, et al., 1983), forcing calcium out of the cells thus forcing them to relax, and opening the user's airways to allow easier breathing. Salbutamol (Ventalin™, Salamol™) has been a popular treatment for asthma and COPD since 1968 (Icha, 2007), while Salmeterol (Serevent™) was introduced in 1988 as a longer lasting alternative (Ullman & Svedmyr, 1988).

Fluticasone propionate (Flixotide™) is an artificial corticosteroid that assists breathing by reducing inflammation in the lung lining (Harding, 1990). Whilst steroids are useful in managing respiratory conditions, deposition of the drug in the oropharynx suppresses the local immune system, and patients often suffer from mouth and throat infections such as oral candidiasis as a result (Lee, et al., 2012), (Renner, et al., 2012). Fluticasone propionate is also supplied as a combination inhaler with salmeterol xinafoate (Seretide™) due to their complementary modes of action (Woolcock, et al., 1996) (Chapman, et al., 1999) (Calverley, et al., 2003). Pure compounds rather than mixtures were used in this study.

Ciclesonide (Alvesco™) is a recently developed inhaled corticosteroid used as a treatment for asthma, hay fever and other respiratory ailments. In order to reduce the mouth and throat infections associated with respiratory steroid application, ciclesonide is designed to be biologically inactive until it interacts with esterase enzymes present in the lung (Mutch, et al., 2007) at which point it is hydrolysed to the active form desisobutyryl-ciclesonide; these enzymes are not found in

the oral cavity to the same extent, and hence the potential benefit of reduced oropharyngeal side effects.

Inhalable drugs are predominately administered by nebuliser, dry powder inhaler (DPI) or by pressurised metered dose inhaler (pMDI). Powered nebulisers have been in use since the 19th century (Sanders, 2007), while cheaper and more portable pMDIs were invented in 1955 (Purewal & Grant, 1997). The ban on CFC propellants following the introduction of the Montreal Protocol (UNEP, 1987) did not include pMDIs due to their medical necessity, but the move away from CFCs did result in a rapid expansion of DPI devices as an alternative to pMDIs (Clark, 1994). However, DPI devices typically require a greater patient inhalation effort in order to disaggregate the powder bed, making them unsuitable for patients with severe respiratory disease. Providing patients are correctly trained on coordinating actuation and inhalation, pMDI devices overcome the disadvantages of DPI devices, and the pMDI is now the most popular device for delivering drugs to the human respiratory system in Britain (Lavorini, et al., 2011). While nebulisers were believed to be more effective than pMDIs in delivering bronchodilator drugs, a double-blind clinical study found them to be no more effective than simpler, cheaper pMDIs with spacers designed for use with babies and toddlers, the hardest age group to administer inhalable drugs to (Delgado, et al., 2003).

Modern pMDIs contain solid drug particles which are suspended in a liquefied hydrofluoroalkane propellant: most commonly HFA-134a (Cripps, et al., 2000) (Leach, 2005). Other co-solvents such as ethanol or oleic acid can be used depending on the drug (Bell & Newman, 2007). The solvent rapidly evaporates at ambient temperature upon activation of the pMDI, generating a fixed dose, inhalable aerosol of micron-sized solid drug particles travelling at a wide range of planar velocities into the user's trachaea and lungs (Crosland, et al., 2009).

1.2 Significance of relative humidity and temperature on delivery efficiency

Drugs acting within the respiratory tract are only effective if the particle aerodynamic diameters are in the 1-5µm range since larger particles cannot reach the receptor sites inside the lungs (Labiris & Dolovich, 2003). Hygroscopic particles can change size as they collect water from the air (Broday & Georgopoulos, 2001) which means that particles manufactured in the correct size range may be too large to be effective by the time they reach the lungs.

Previous work has shown (Tong, et al., 2014) that salbutamol sulfate deliquesces at around 92% relative humidity (RH). Deliquescence describes the phase change of a crystalline solid to a saturated solution droplet using water condensed from the surrounding air. Temperature can affect the RH level required to bring about deliquescence in hygroscopic substances but the effect varies between compounds (Lipasek, et al., 2013). Temperature also has a significant influence over the saturation water vapour pressure of air (Lawrence, 2005) so the air inside the lungs at 37^{o}C and near-100% RH contains three times the concentration of water as outside air at similar RH and 20^{o}C (Nave, 2004). However, temperature influences the kinetics of drug dissolution only, rather than the thermodynamic behaviour of solid particles, which remain relatively unchanged, and it is not expected to significantly impact hygroscopic properties.

The rate of deliquescence dictates the rate of adsorption of drugs across lung epithelia, since a given drug cannot be absorbed until it has fully dissolved (Bikiaris, 2011). This lends a time-critical aspect

to drug delivery since solid particles in the lungs are removed over time by macrophage and mucociliary activity (Hardy & Chadwick, 2000). If, for example, 80% of a given drug is removed in this manner before it can perform its function, five times the dose must be administered and resultant side effects such as immunosuppression with corticosteroids (Lee, et al., 2012) and hypoalkaemia with salbutamol (Hung, et al., 1999) have a greater impact on patient health. On the other hand, as mentioned in the previous section rapid deliquescence can lead to an increase in particle size that makes it more difficult for drugs to reach deep enough into the airways. Finding optimal values for both particle size and hygroscopicity is essential to providing patients with the most effective treatment with the least side effects, and is the primary motivation for this series of experiments.

Investigations are ongoing into the hygroscopic behaviour of drug aerosols delivered by nebuliser (Haddrell, et al., 2014). However, the popularity of pMDI delivery for bronchodilation medication and the logistical difficulties involved in modelling the pharmacokinetic behaviour of medication inside the lung of a living creature mean that similar studies on pMDI-delivered drugs are justified.

This series of experiments investigates the use of an optical trap to stably levitate drug aerosols released by popular pMDI devices. The set up allows for the control of temperature and RH to more closely mimic the human lung than conventional cover slip analysis.

2. Methods and Materials

The combination of optical trap, Raman spectroscopy and model lung was first described in Tong et al 2014 (Tong, et al., 2014). The optical trap uses a counter propagating dual beam (CPDB) trap configuration first described by Rkiouak et al. (Rkiouak, et al., 2014) and deployed in several subsequent experiments (Tang, et al., 2014) (Jones, et al., 2015) (Hunt, et al., 2015). This trapping setup is remarkable because it is capable of stably trapping micron-sized solid particles of non-spherical geometry for periods of time up to several hours.

2.1 Counter propagating dual beam optical trap

The trapping beams were generated by a 1064nm Nd:Yag laser (Ventus, Laser Quantum) passed through a beam splitter (Oz optics) and fibre-coupled into two single-mode fibres. Each fibre output was delivered to beam expansion and collimation optics before entering the objective lenses. The laser power at output was 15mW from the top objective lens and 10mW through the bottom objective lens [fig 2]. The asymmetry in power ensured that trapped particles were driven closer to the optical focus plane of the bottom objective through which the Raman laser is passed, ensuring better focus on the resulting images (Rkiouak, et al., 2014). The foci of the lasers were positioned ~10µm apart, which created a trapping volume large enough to stably hold 1-5µm particles for long periods. Once all useful observations had been collected from a trapped particle, the particle was allowed to fall under gravity to the cover slip by blocking the 1064nm trapping beams.

There are several reasons to prefer an optical trap to cover slip analysis. The most significant is that pharmaceutical aerosols are, until they reach the respiratory tract, suspended particles and attempts to recreate their conditions should be as close as possible. Interactions between collecting substrates and water can measurably alter the deliquescence point of hygroscopic particles (Eom, et al., 2014) with hydrophobic surfaces like glass reducing the deliquescence point of sodium chloride by 1.5% compared to a suspended particle. Any particle landing on a cover slip will have part of its

surface in contact with the slip rather than exposed to the surrounding air [see figure 1], so a hygroscopic particle will form a water layer beginning with a halo around the contact point with the cover slip rather than across the surface dictated by the particle's geometry and density of hygroscopic sites. The shape of the resulting droplet and rate of adsorption will both be affected by the presence of a cover slip.

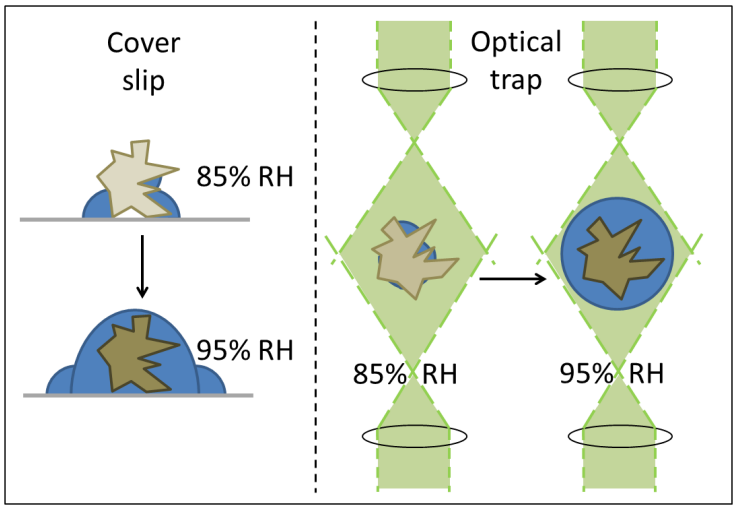

Figure 1. An illustration of the influence of coverslips on the formation of water layers on hygroscopic particles

This is especially important in time-critical experiments such as those reported in this paper. Optical trapping represents the best current option for making detailed observations of physical and chemical changes on suspended particles in varying conditions, and yields better resolved Raman spectra than particles observed on a cover slip due to the removal of interfering spectral features associated with the composition of the cover slip. Optical trapping is superior for single particle spectroscopy when compared to other single particle levitation techniques, such as electrodynamic balances or acoustic trapping, because the optical setup ensures good alignment between the studied particle and spectroscopic probe (Hargreaves, et al., 2010).

Optical trapping is easiest with spherical or spheroidal particles and droplets due to their symmetry (Ashkin, 1992). While the setup used in this work has demonstrated the capacity to trap non-spherical particles for periods of an hour or longer (Rkiouak, et al., 2014) (Tong, et al., 2014), particles that are closer to spheres are still easier to trap for the same reasons.

2.2 Raman Spectroscopy

Raman spectroscopy is a powerful technique for examining the functional groups and intermolecular interactions of substances, requiring very small sample masses and no sample preparation (Hirschfeld & Chase, 1986) (Vankeirsbilck, et al., 2002) and making it ideal for the analysis of micrometer-scale drug particles. Raman spectroscopy has much lower signal-to-noise ratio than competing infrared analysis techniques because of the visible range detection region, and because the scattering wavelengths are separate from those of the excitation laser, so the technique can be effective with very small samples whose absorption would be indistinguishable against a standard FT-IR beam (PerkinElmer Inc, 2008). These experiments use a Raman setup which collects back-

scattered photons along the same path as the excitation laser, but filtering the excitation photons with a Razoredge dichroic mirror and longpass edge filter combination (SemRock) (Figure 2b).

Raman scattering was generated using a 514.5nm Ar-ion laser (Innova 300C, Coherent), with a power of 4.3mW measured at the laser focus. Each Raman spectrum was generated by a 30 second exposure to the 514.5nm laser. These wavelength and power settings were selected based on previous experiments (Hunt, et al., 2013) as they were found to cause minimal heating of samples over long periods of exposure. It is known that organic molecules with multiple conjugated double bonds can fluoresce when exposed to UV-visible light frequencies (Sauer, et al., 2011) and this fluorescence can saturate the comparatively weak Raman scattering signal (Huang, et al., 2003). This effect is discussed in section 3.2d. Raman scattered light was collected in the region of 540-1830 cm^{-1}.

Wavelength calibration of the Raman spectrometer was carried out using a cover slip with raised sides containing pure liquid toluene. The position of spectral peaks for toluene is well characterized and these are used as a reference for wavelength calibration.

2.3 Artificial Lung Chamber & Particle Imaging

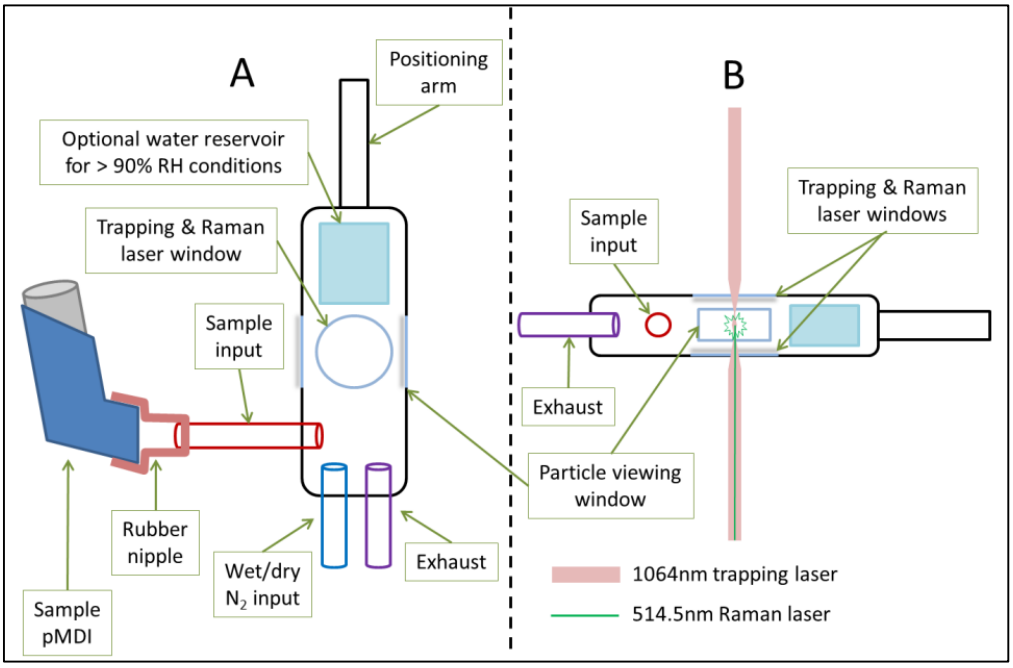

Figure 2 Top-down (A) and side (B) views of the artificial lung chamber
(High RH conditions here defined as >93% @ 20°C)

The artificial lung (figure 2) was an aluminium chamber of internal dimensions approximately 10 x 2 x 1cm, with borosilicate cover slip windows at the top and bottom to admit laser light and also at the sides to observe particles using a Mitutoyo M Plan Apo 20x objective lens connected to a CCD camera (Princeton Instruments, Spec10), opposite an LED source (Comar Optics). A monitor attached to the CCD camera allowed users to observe particles passing around, through and into the optical trap.

Relative Humidity (RH) and temperature were monitored using a Sensirion SHT-75 RH probe with a manufacturer-stated accuracy of ±1.8% RH and ±0.3°C. Raman spectra were collected within 3 minutes of reaching the desired RH. RH levels were altered using N_2 gas sourced from boiled off liquid nitrogen, using a flow rate of ~200 cm^3/min through a Bronkhorst MV-301 mass flow controller. A lower flow rate of 100 cm^3/min was used for RH adjustment of the Salmeterol particles, since higher flow rates tended to dislodge the particles from the trap for reasons discussed in section 3a. The input and exhaust ports were located on the same face of the cell in order to generate slow flow conditions around trapped particles and thus minimise turbulence that might dislodge the particle.

The gas was either run into the cell directly (low RH) or passed through a bubbler containing milli-Q grade deionized water before entering the cell (high RH). For very high RH conditions, a water reservoir was added inside the chamber. While the bubbler could provide RH up to ~90%, the reservoir could generate RH as high as 93% at 30°C and up to 98% at 20°C.

Salmeterol, fluticasone and ciclesonide were analysed at ambient temperature at high and low RH. Salbutamol sulfate was analysed both at ambient temperature and at more physiologically relevant temperatures by incubation of the microscope environment using Solent Scientific incubator components.

2.4 pMDI injection

To dispense the aerosolised drug into the artificial lung chamber, a simple connector was built for the pMDI outlet involving a flexible rubber cap with a rigid 6mm (internal diameter) PTFE tube protruding through it. The tube was connected to a similar tube on the side of the artificial lung by a short length of flexible silicone tubing. The funnel was washed sequentially in deionized water and methanol to minimise potential cross-contamination with other drugs.

The propellant flow within the sample chamber carried material from each pMDI discharge into the path of the trapping beam. Drug particles passing across the side viewing window were illuminated by an LED and observed on a monitor. Scattering of the unfiltered trapping laser from a trapped particle was viewed on the same monitor to indicate the positional stability of the particle.

Based on the stated mass per release of each drug, the density of the solid material (Zhejiang NetSun Co., Ltd., 2010), the assumption that an average particle is solid and has a volume of approximately 10μm^3, a single release from each inhaler is estimated to deliver 10^6 to 10^7 particles to the chamber, although some are assumed to be lost by impaction onto the walls of the chamber. A single trapped particle at least 2µm in diameter is sufficient to generate a Raman spectrum.

2.5 SEM imaging

Each drug was actuated onto a glass cover slip and coated with 10nm gold particles in a Polaron SC7640 sputter coater. The cover slips were attached to Agar Scientific 25mm double sided sticky carbon tabs prior to imaging on a Philips XL30 ESEM FEG. [Haijie says – more detail?]

2.6 Chemical Structures of the asthma drugs investigated

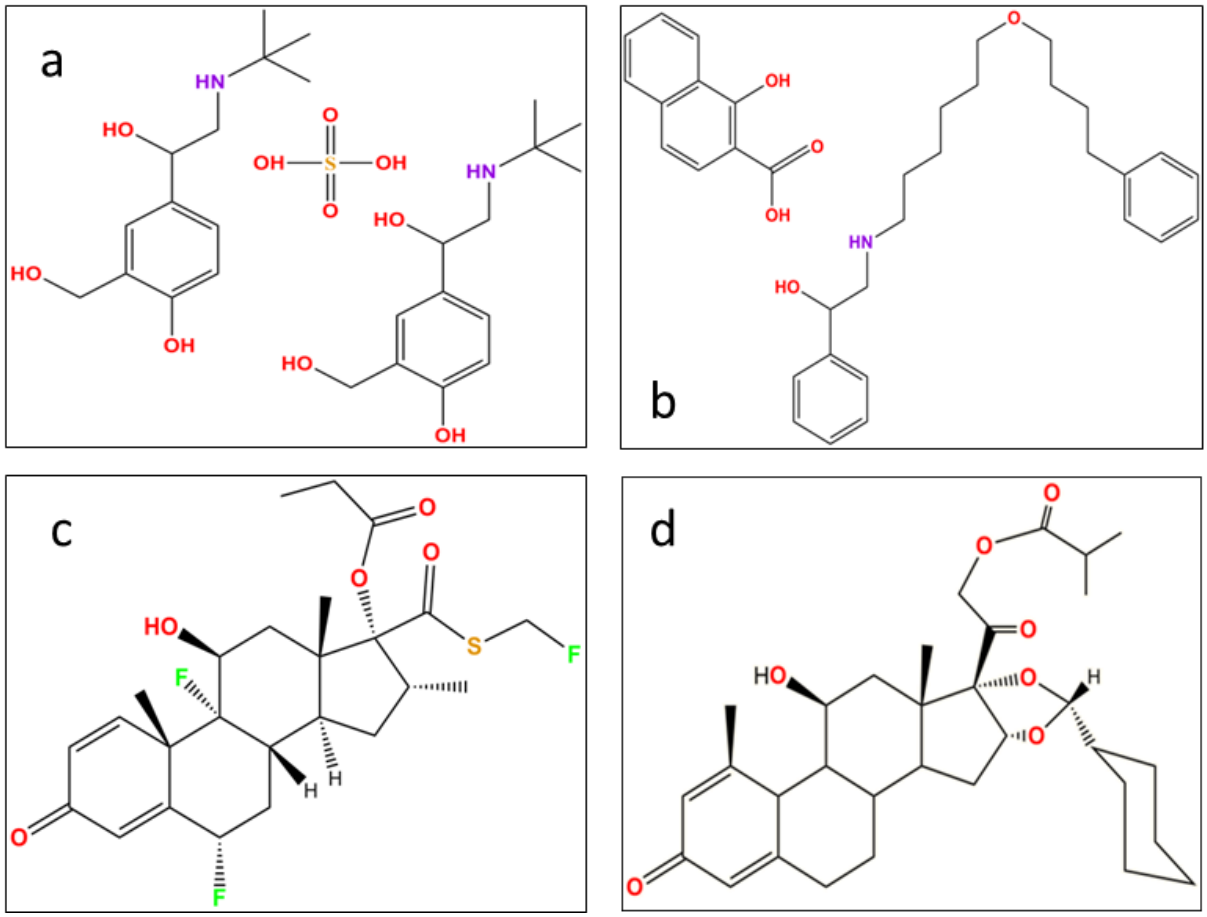

Figure 3 Chemical structures of single molecules of salbutamol sulfate (a), salmeterol xinafoate (b), fluticasone propionate (c), and ciclesonide (d)

Salbutamol sulfate particles were generated from a Salamol brand inhaler by Ivax Chemicals ltd. Salbutamol sulfate contains several polar groups and no long aliphatic chains, and its hygroscopic character was already documented (Tong, et al., 2014). Salmeterol xinafoate particles were produced from a "Serevent" brand inhaler produced by Cipla Ltd. Salmeterol also contains multiple polar groups but also a long aliphatic chain. Its hygroscopic properties are to be determined.

Fluticasone propionate, generated from a "flixotide" brand inhaler, is manufactured by GlaxoSmithKline, and ciclesonide particles were generated by a "Ciclohale" brand inhaler also by Cipla Ltd. Ciclesonide is produced under license from Takeda UK Ltd. Fluticasone propionate and ciclesonide are both steroids and as such are relatively hydrophobic and are not expected to show hygroscopic properties.

3. Results and Discussion

3.1 Thermodynamic Calculations of Particle Hygroscopicity

Using E-AIM to predict the hygroscopic properties of the drug molecules (Clegg, et al., 2001) (Engelhart, et al., 2011) (Ling & Chan, 2008) yielded two distinct types of interaction (figure 4). The beta-2 agonists contain a higher proportion of hydrophilic groups and are thus expected to be strongly hygroscopic, while the more lipophilic steroids are expected to collect little water from the air even under near-100% RH conditions. However, this does not take into account the crystal

structure of solid particles which may block access to hydrophilic sites and prevent otherwise hydrophilic molecules from interacting with water in the air.

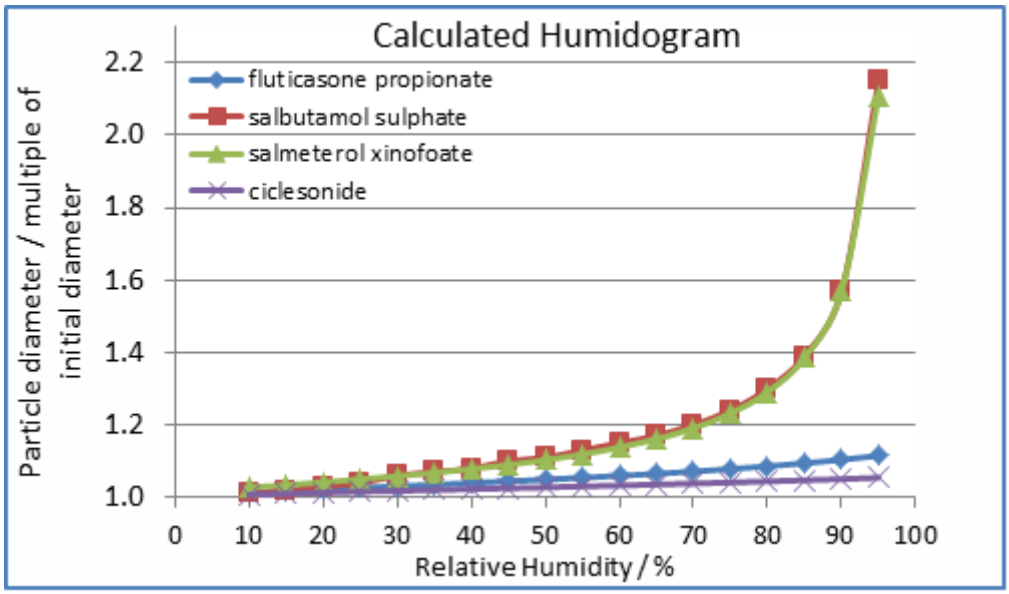

Figure 4 Influence of humidity on particle diameter predicted from chemical bonding

3.2 Drug Particle Crystallography

The Mercury 3.6 program (Macrae, et al., 2006) was used to simulate the crystal structure of all drugs whose structures had been added to the Cambridge Structural Database run by the Cambridge Crystallographic Data Centre (CCDC, 2015).

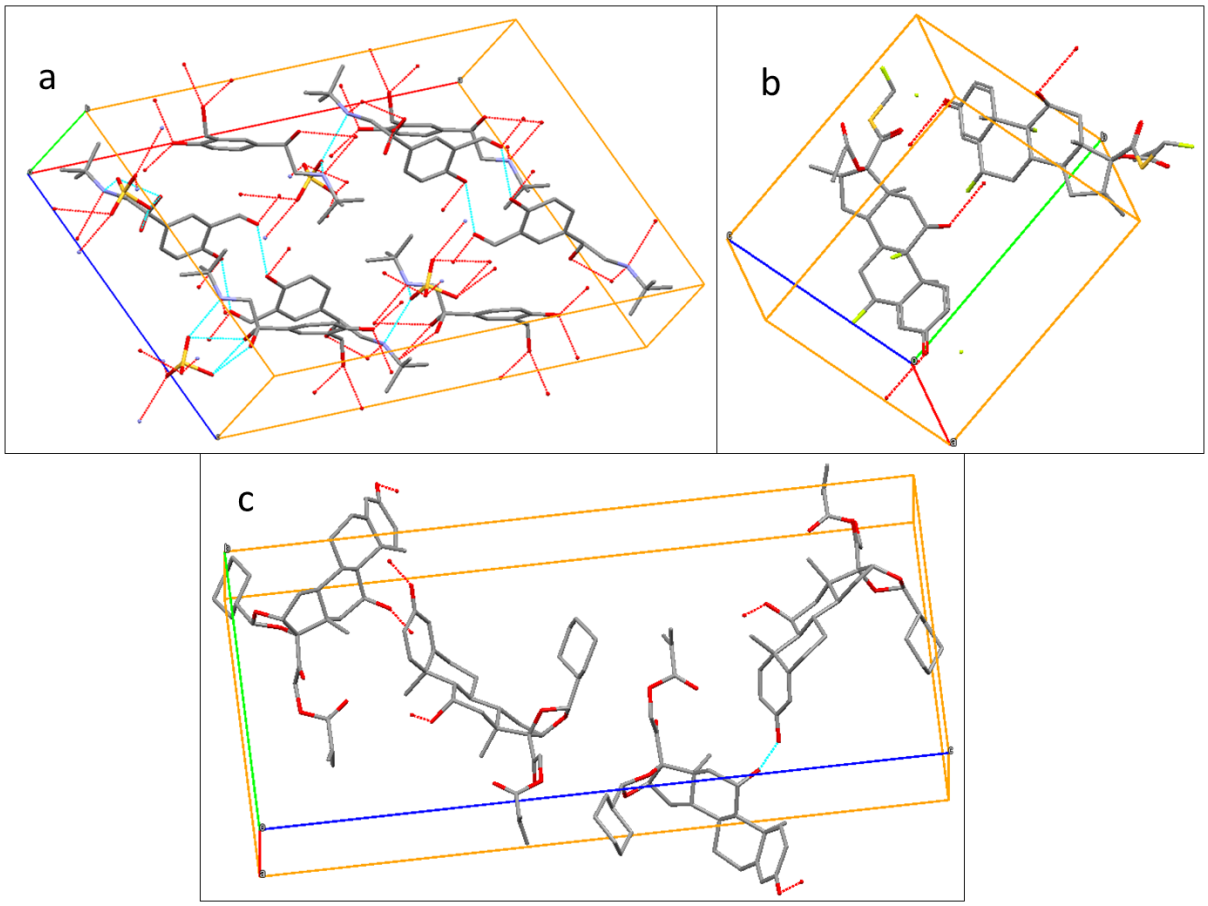

Figure 5 Model unit cells of salbutamol sulfate (a), fluticasone propionate (b), and ciclesonide (c). Salmeterol xinafoate's unit cell was not available at time of writing. Hydrogen bonding within the unit cell is illustrated with a cyan line, while hydrogen bonding external to the unit cell (thus contributing to hygroscopic behaviour) are illustrated with red lines.

The chemical structure of salbutamol sulfate (figure 5a) shows hydrophilic sites across the molecule, which are indicated in Figure 5 as red lines symbolizing hydrogen bonding capability of the structure. The most likely crystal form generated by rapid solvent evaporation in air was first described in 1978 (Leger, et al., 1978), with an 8 molecule unit cell (figure 5a) that shows hydrogen bonding sites on every face. Hygroscopic behaviour is inferred from this structure and has been demonstrated in previous experiments at room temperature (Tong, et al., 2014).

Salmeterol is not found in the Cambridge Structural Database. Solid structures are variously described as either amorphous, or needle-like or plate-like crystals depending on the exact conditions of manufacture (York & Hanna, 1994) (Barjoan & Clotet, 2009). Salmeterol xinafoate is bound together by hydrogen bonding of the δ-positive amine group on salmeterol to the δ-negative carboxylic acid group on the xinafoic acid. The two groups are expected to cancel their respective charges, leaving few hydrophilic sites open to interaction with water while the particle is in a solid state.

As a steroid, fluticasone is expected to be lipophilic (Lipworth & Jackson, 2000). The structure of fluticasone (figure 5b) does have a number of polar groups. However, the documented crystal structure (Cejka, et al., 2005) describes a plate-like structure with any hydrogen bonding occurring along the plane of growth (figure 5b) resulting in water interaction only along edges, and likely to result in little or no hygroscopic behaviour.

Ciclesonide (figure 5c) is found as either needle-like (Phull, et al., 2012) or needle-like and spherulitic crystals as well as amorphous solids (Feth, et al., 2007) depending on solvent type and evaporation time. Ciclesonide has multiple polar groups but the model unit cell described by Feth et al. (2007) describes most of the oxygens arranged inside the crystal with the hydrophobic sites facing outward. Limited hydrogen bonding due to the hydroxyl and ketone groups on adjacent molecules have the potential to attract water molecules to crystal faces, but the hydrophobic nature of the rest of the exposed molecule implies that hygroscopic behaviour is unlikely.

3.3 SEM imaging and Trapping Logistics

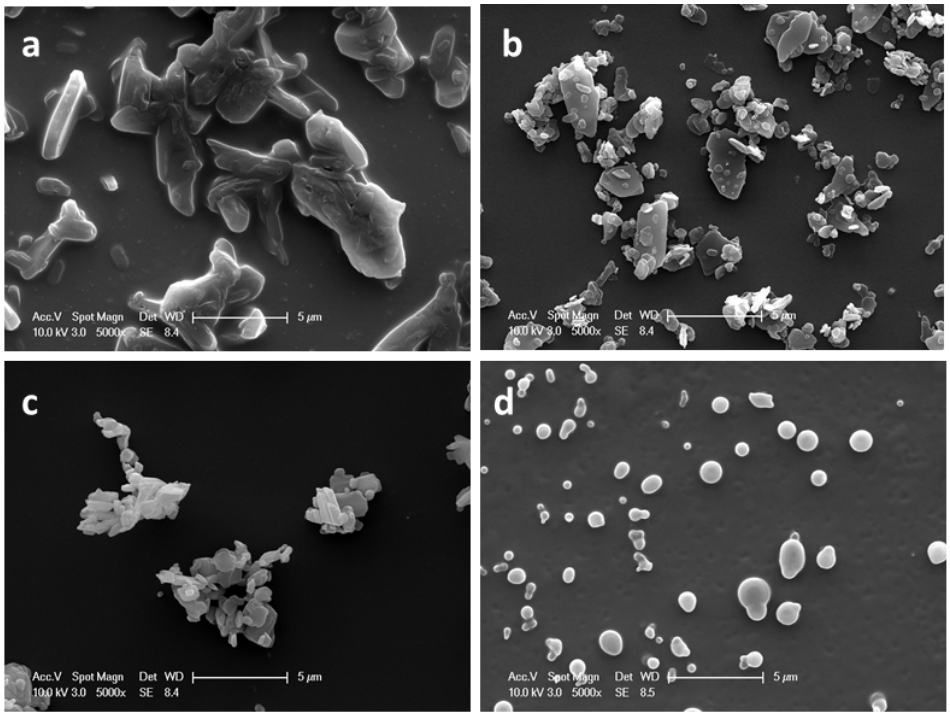

Figure 6 SEM images of: (a) salbutamol sulphate, (b) salmeterol xinafoate, (c) fluticasone propionate & (d) ciclesonide

The likelihood of a particle being successfully trapped was dictated by both particle shape and the number of particles generated per release. Salbutamol sulfate had been optically trapped previously on the same apparatus (Tong, et al., 2014). The thick, needle like shape of salbutamol particles (fig 6a) is well suited to entrapment for reasons detailed in section 2.4, and the 100µg per release dose of the available inhalers resulted in a successfully suspended particle roughly once for every other release. Salmeterol xinafoate was significantly harder to trap and retain than the others due to a combination of its low dose (20µg per release) and flat, platelike aggregate structure (fig 6b). Fluticasone has a similar crystal structure to salmeterol but a much higher dose (250µg per release) and was more reliably trapped than salbutamol sulfate (fig 6c). Ciclesonide was similar in trapping efficiency to fluticasone since its lower dose (160µg per release) was balanced by a more spherical particle shape (fig 6d).

3.4 Raman spectrum changes from hygroscopic properties and additional compounds

Hydrogen bonding with water molecules adjacent to the polar groups of organic molecules expands the range of vibrational energy states that can generate Raman scattering photons. This effect allows water uptake by hygroscopic particles to be monitored by Raman spectroscopy.

All four drugs use hydrofluoroalkane HFA 134a/Norflurane as a propellant. The salbutamol and ciclesonide inhalers also report anhydrous ethanol among their ingredients. Norflurane contains four C-F bonds, each of which generate a distinctive Raman scattering peak at 1234 cm^{-1}. This peak is not expected to be visible in the Raman spectra of the drug molecules, apart from Fluticasone which has 3 C-F bonds of its own, due to Norflurane's low boiling point (-26.5^{o}C, (Lide, 1991)) at atmospheric pressure causing all of the propellant to boil off before readings can be collected. The spectra collected from particles other than fluticasone do not show peaks in the C-F stretching region, which implies that all propellant boils off before the particles are scanned.

3.5 Salbutamol sulfate / Salamol™

3.5a Raman spectra and structural information

Salbutamol sulfate contains fewer distinctive functional groups than the other drugs. Each salbutamol molecule contains a single phenol group, two aliphatic hydroxyls and a secondary amine. One molecule of salbutamol contains two ionised salbutamol molecules bound to a single sulfate group. The S=O symmetric stretches on the sulfate show a small but distinctive peak at 1154 cm^{-1}. The largest peaks in the salbutamol spectrum correspond to –CH wagging at 656 cm^{-1}, aromatic ring vibration at 752 cm^{-1}, C-C-O stretches in relation to the aliphatic hydroxyls at 784 cm^{-1}, asymmetric hydroxyl stretches at 969, 977 and 1008 cm^{-1}, phenyl ring vibrations at 1059 and 1074cm^{-1}, a prominent CH stretch at 1257cm^{-1} (this bond can be found in figure 3a just above the ring) CH_2 and CHOH vibrations again from the aliphatic hydroxyls at 1360 cm^{-1}, a broad ring stretching peak around 1450cm^{-1} followed by a CH_2-N amine peak at 1463cm^{-1}, and finally a strong peak at 1615cm^{-1} corresponding to the phenolic C-OH stretch. These peaks correspond to those found in the literature (Ali, et al., 2009).

3.5b Impact of RH and Temperature on salbutamol spectra

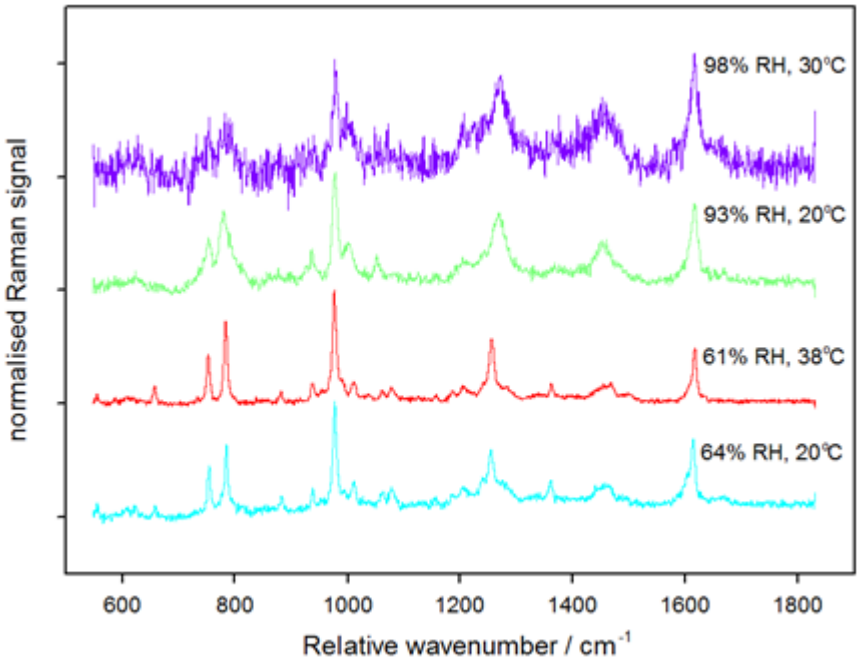

Figure 5 Raman spectra of optically trapped salbutamol sulfate particles at a range of RH and temperatures

RH above 92%, the deliquescence point identified by Tong et al. (Tong, et al., 2014), could not be maintained at physiological temperature (37°C) with the available equipment, so measurements were taken at 30°C- the highest temperature at which >92% RH could be maintained. The particle trapped at 98% RH and 30 °C was small, hence the poorer signal/noise ratio. The contrast between the relatively dry and relatively wet particles is clear to see as the peaks of the wet particles are broader, and some peaks such as the hydroxyl peak at 1008cm^{-1} and the amine peak at 1463cm^{-1} are more pronounced. The more pronounced peak around the aliphatic hydroxyl stretches near 800cm^{-1} is the result of an overlapping fluorescence signal seen in aqueous solutions of salbutamol (Dodson, et al., 2011) (Pandya, et al., 2010) and is consistent with Tong et al's findings (Tong, et al., 2014).

The spectral traces of similar RH but contrasting temperature are very similar. This implies that the temperature difference from the open air to inside the user's body is not great enough to cause changes in the hygroscopic properties of Salbutamol. Relative humidity is thus shown to be the major factor controlling the particle's hygroscopicity.

3.6 Salmeterol xinafoate / Serevent™

3.6a Raman spectra and structural information

Salmeterol xinafoate contains several aromatic rings, an ether group, a benzoic acid and a secondary amine. Benzoic acid is distinct from both aromatic rings and carboxylic acids due to the increased conjugation (Kwon, et al., 1994) and shows distinctive peaks in the solid state at 1627 cm^{-1}, 994 cm^{-1} and 788 cm^{-1}. These peaks are all present in our spectra (see figure 7). Ring stretches are clearly visible at 1580-1616 cm^{-1}, 1400-1420 cm^{-1} (the multiple strong peaks denoting ring stretches shifted by the various adjacent functional groups) and symmetric ring stretches are visible at 1000-1028 cm^{-1}, 1215 and 1257 cm^{-1}. A strong amine vibration peak is visible at 1204 cm^{-1}. A sharp peak at 730 cm^{-1} corresponds to rotational peaks from CH_2 groups, as would be expected by a molecule with a long

aliphatic chain like salmeterol. The ether group can be identified by small peaks at 554 and 1145 cm^{-1}. These spectra correspond well with previously published, well-defined Raman spectra (Ali, et al., 2008a).

3.5b Impact of RH on salmeterol spectra

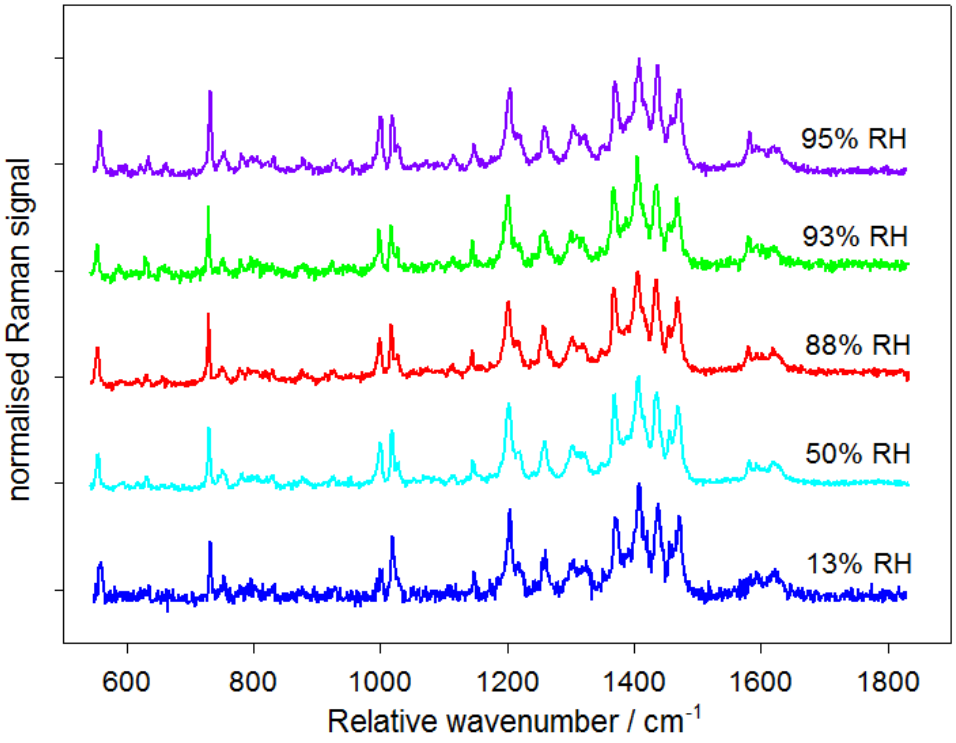

Figure 7 Raman spectra of salmeterol xinafoate at a range of RH values

The hygroscopic behaviour of salmeterol xinafoate predicted by E-AIM may be limited by stearic hindrance of the hydrophilic sites by hydrophobic structures arranged around them in solid crystals. Salmeterol xinafoate does not demonstrate any visible broadening around peaks corresponding to either salmeterol's amine group or the carboxylic acid group on its xinafoic acid partner upon RH enhancement. However, the relative enhancement of peaks corresponding to aromatic ring stretches at 650, 1000 and 1580 cm^{-1} imply some interaction with water around some or all of the aromatic rings in salmeterol xinafoate at >88% RH.

3.4 Fluticasone propionate / Flixotide

3.4a Raman spectra and structural information

Fluticasone contains several distinctive bonding types that would be expected to yield distinctive peaks in any resulting Raman spectra: a phenone, an ester, a thioether and three C-F bonds across the molecule. Fluticasone has been imaged by Raman spectroscopy previously and its spectra interpreted in depth (Ali, et al., 2008b) (Rogueda, et al., 2011) (Theophilus, et al., 2006) (Wang, et al., 2014), which provides useful references for the spectra generated here.

The most distinctive aspect of our fluticasone spectrum was the sharp peak at 640 - 650 cm^{-1}. The peak overlaps the thiocarboxylic ester peak found at 646cm^{-1} in the literature (Coates, 2000) (Bloxham, et al., 2002), but was much more intense and varied in intensity across different particles.

This peak was believed to be a result of a second harmonic resonance effect from the 1064 nm trapping laser, as a 532 nm excitation would result in a resonance peak at 639.5 cm^{-1}.

Repeated measurements of fluticasone particles on a coverslip with the 1064 nm trapping laser off did not show the peak in the Raman spectrum, and the peak did not appear when the 1064nm laser was turned on at powers equivalent to those used in the optical trap. However, at higher power outputs the same peak observed in trapped particles began to appear and to dominate the Raman spectrum. The resonance peak is stronger in symmetrical particles that are more likely to be stably trapped so more pronounced peaks in the Raman spectra of trapped fluticasone are to be expected. The spectra shown in figure 8 have had the 640-650 cm^{-1} region normalised to remove the resonance peak.

The strongest peak in the spectrum of fluticasone is the C=O vibration at 1659cm^{-1}, followed by the $–CH_3$ symmetric stretch (there are 4 $–CH_3$ groups in Fluticasone) at 1606cm^{-1}. $–CH_2$ and –CH stretches occur at around 1380 and 1330 cm^{-1} respectively and highly distinctive C-F and S-C-F bands occur at 1234cm^{-1} and 1022cm^{-1}. As expected, this was the only compound that exhibited scattering consistent with C-F bonds, implying that in all samples the Norflurane propellant had boiled off prior to analysis. The phenone group registers as an OOH/CCH aromatic deformation peak at 888cm^{-1}. A small C-H wagging peak can be seen at around 700cm^{-1}.

3.4b Impact of RH on fluticasone spectra

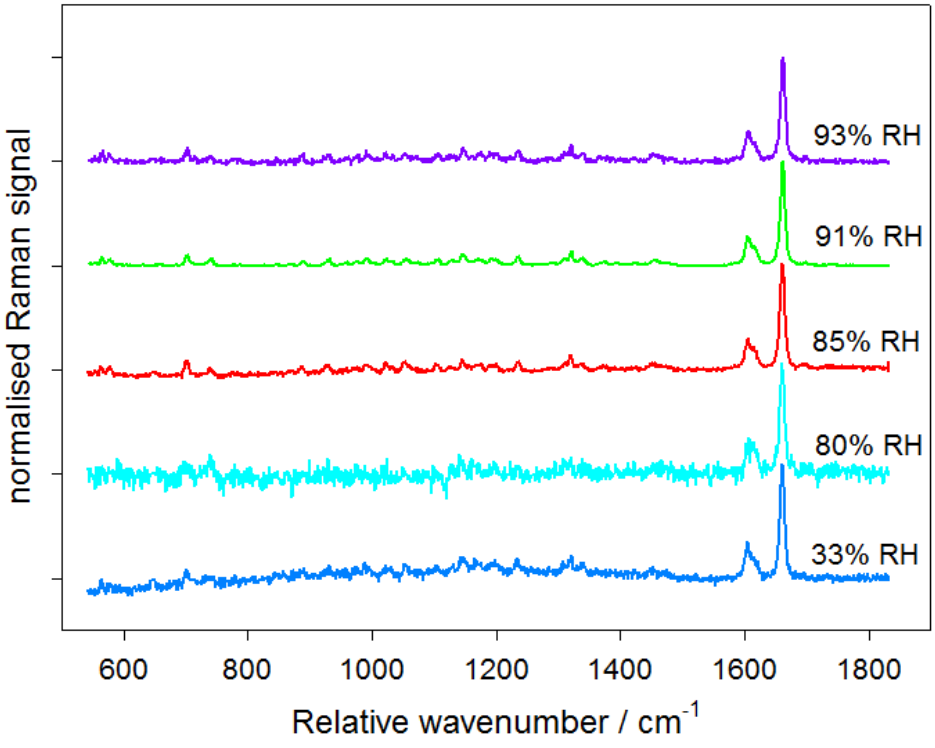

Figure 8 Raman spectra of fluticasone propionate at a range of RH values

The spectrum collected at 80% RH was from a small particle- around 1µm in diameter. This accounts for the greater noise in the signals. Otherwise, no peaks are displaced or strongly deformed by the rise in relative humidity.

3.5 Ciclesonide / Alvesco™

3.5a Raman spectra and structural information

Ciclesonide (Feth, et al., 2008) has a diverse selection of functional groups, which generates a complicated Raman spectrum. The largest peak at 1654cm^{-1} represents the stretching vibration of an α, β-unsaturated carbonyl, while the adjacent peak at 1601cm^{-1} shows the neighbouring C=C bond. Ciclesonide contains four -CH_3 groups and this corresponds to another large, broad peak at 1443cm^{-1}. The three ether bonds generate another large peak at 1112cm^{-1}, and the single ester linkage appears at 1242cm^{-1}. Ciclesonide has a single hydroxyl group attached to a six-membered saturated ring, and a matching "cyclic alcohol" stretch appears at 1029cm^{-1}. The C-C stretches of the two saturated six-membered rings are found at 963cm^{-1}. Multiple small peaks around 800-900cm^{-1} represent ring deformation in the phenol group adjacent to the saturated rings. Another region of small peaks around 1330cm^{-1} corresponds to the various symmetric and antisymmetric stretches of the isopropyl group.

3.5b Impact of RH and Temperature on Ciclesonide Spectra

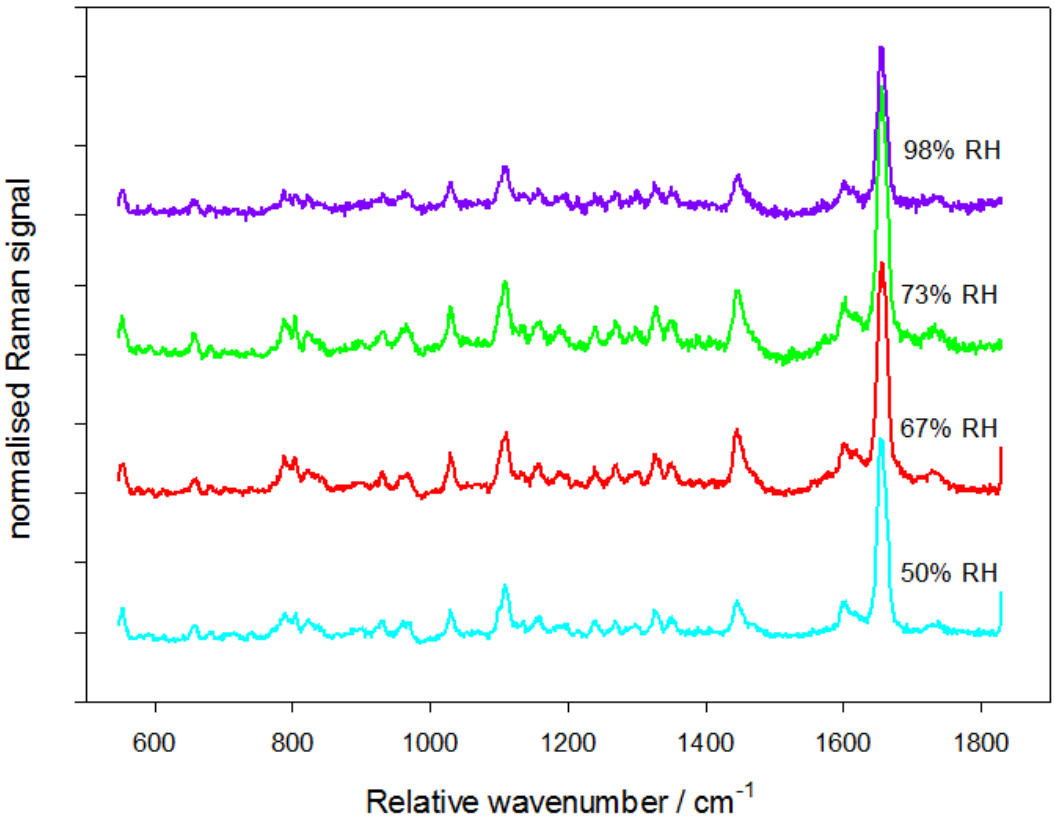

Figure 9 Raman spectra of ciclesonide at a range of RH values

As a steroid, ciclesonide is not very hydrophilic and does not contain many polar groups. The crystal structure shows very little opportunity for water uptake on surfaces. It would not be expected to show hygroscopic behaviour, and no such behaviour was observed as all Raman spectra shown in Figure 9 show not changes from low to high humidities between 50-98% RH.

4. Conclusions

The Raman spectra of four optically trapped drug particles (salbutamol sulfate, salmeterol xinafoate, fluticasone propionate and ciclesonide) were measured within a model lung. The model lung allowed for modification of local relative humidity (RH) to test the drugs for hygroscopic behaviour, while the optical trap eliminated any potential surface artefacts from water droplets forming around a solid particle on a cover slip. Raman spectroscopy allowed for the direct observation of the hydrogen bonding with water in hydrophilic groups, where the broadening of peaks indicates hygroscopicity.

The hygroscopic properties of salmeterol, fluticasone and ciclesonide are not influenced to a measurable degree by changes in RH from 30% (similar to the open air in average weather conditions) to 93-95% at 295^{o}K …. . Future experiments will discern whether biologically relevant temperatures and, ideally, RH values closer to 100% trigger deliquescence and over what timescale. The observed fluorescence effects of the Raman laser on salmeterol xinafoate may be avoided in future by using a longer excitation wavelength Raman probe.

Salbutamol sulfate particles, meanwhile, are affected by changes in RH and change size when exposed to very humid air. Thus a reduction in average particle size at the point of manufacture based on the hydrated rather than dry diameter might yield the same medical response from a lower dose.

Works Cited

Ali, Edwards, Kendrick & Scowen, 2008b. Vibrational spectroscopic study of fluticasone propionate. *Biomolecular Spectroscopy,* pp. 244-247.

Ali, Edwards, Kendrick & Scowen, 2009. Vibrational spectroscopic study of salbutamol hemisulphate. *Drug Testing and Analysis,* pp. 51-56.

Ali, et al., 2008a. Vibrational spectroscopic characterisation of salmeterol xinafoate polymorphs and a preliminary investigation of their transformation using simultaneous in situ portable Raman spectroscopy and differential scanning calorimetry. *Analytica Chimica Acta,* pp. 103-112.

Ashkin, 1992. Forces of a single-beam gradient laser trap on a dielectric sphere in the ray optics regime. *Biophysical Journal,* pp. 569-582.

Barjoan & Clotet, 2009. Spain, Patent No. EP2127641A1.

Bell & Newman, 2007. The rejuvenated pressurised metered dose inhaler. *Expert Opinion on Drug Delivery,* pp. 215-234.

Bikiaris, 2011. Solid dispersions, Part I: recent evolutions and future opportunities in manufacturing methods for dissolution rate enhancement of poorly water-soluble drugs. *Expert Opinion on Drug Delivery,* pp. 1501-1519.

Broday & Georgopoulos, 2001. Growth and Deposition of Hygroscopic Particulate Matter in the Human Lungs. *Aerosol Science and Technology,* p. 144–159.

Calverley, et al., 2003. Combined salmeterol and fluticasone in the treatment of chronic obstructive pulmonary disease: a randomised controlled trial. *The Lancet,* pp. 449-456.

CCDC, 2015. *WebCSD v1.1.1.* [Online]
Available at: http://webcsd.cds.rsc.org/index.php
[Accessed 10 11 2015].

Cejka, Kratochvil & Jegorov, 2005. Crystal Structure of Fluticasone Propionate, C25H31F3O5S. *Zeitschrift für Kristallographie - New Crystal Structures,* pp. 143-144.

Chapman, et al., 1999. Salmeterol and fluticasone propionate (50/250 microg) administered via combination Diskus inhaler: as effective as when given via separate Diskus inhalers.. *Canadian Respiratory Journal: Journal of the Canadian Thoracic Society,* pp. 45-51.

Clark, 1994. Medical Aerosol Inhalers: Past, Present, and Future. *Aerosol Science & Technology,* pp. 374-391.

Coates, 2000. Interpretation of Infrared Spectra, A Practical Approach. In: *Encyclopedia of Analytical Chemistry.* Chichester: John Wiley & Sons Ltd, pp. 10815-10837.

Cripps, Riebe, Schulze & Woodhouse, 2000. Pharmaceutical transition to non-CFC pressurized metered dose inhalers. *Respiratory Medicine,* 94(2), pp. S3-S9.

Crosland, Johnson & Matida, 2009. Characterization of the spray velocities from a pressurized metered-dose inhaler. *Journal of Aerosol Medicine and Pulmonary Drug Delivery,* pp. 85-97.

Delgado, Chou, Silver & Crain, 2003. Nebulizers vs metered-dose inhalers with spacers for bronchodilator therapy to treat wheezing in children aged 2 to 24 months in a pediatric emergency department.. *Archives of Pediatric and Adolescent Medicine,* pp. 76-80.

Dodson, et al., 2011. Photophysical and photochemical properties of the pharmaceutical compound salbutamol in aqueous solutions. *Chemosphere,* pp. 1513-1523.

Engelhart, et al., 2011. Water content of aged aerosol. *Atmospheric Chemistry & Physics,* Issue 11, pp. 911-920.

Eom, et al., 2014. Influence of collecting substrates on the characterization of hygroscopic properties of inorganic aerosol particles.. *Analytical Chemistry,* 4(86), pp. 2648-2656.

Feth, et al., 2008. USA, Patent No. US20100120737 A1.

Feth, et al., 2007. Physicochemical, Crystallographic, Thermal, and Spectroscopic Behavior of Crystalline and X-ray Amorphous Ciclesonide. *Pharmaceutics, Preformulation and Drug Delivery,* pp. 3765-3780.

Haddrell, et al., 2014. Dynamics of aerosol size during inhalation: Hygroscopic growth of commercial nebulizer formulations. *International Journal of Pharmaceuticals,* pp. 50-61.

Harding, 1990. The human pharmacology of fluticasone propionate. *Respiratory Medicine,* pp. 25-29.

Hardy & Chadwick, 2000. Sustained Release Drug Delivery to the Lungs. *Clinical Pharmacokinetics,* pp. 1-4.

Hargreaves, et al., 2010. Measurements of the Equilibrium Size of Supersaturated Aqueous Sodium Chloride Droplets at Low Relative Humidity Using Aerosol Optical Tweezers and an Electrodynamic Balance. *The Journal of Physical Chemistry,* pp. 1806-1815.

Hirschfeld & Chase, 1986. FT-Raman Spectroscopy: Development and Justification. *Applied Spectroscopy,* 08 January.pp. 133-137.

Huang, et al., 2003. Near-infrared Raman spectroscopy for optical diagnosis of lung cancer. *International Journal of Cancer,* pp. 1047-1052.

Hung, Chu, Wang & Yang, 1999. Hypoalkaemia and salbutamol therapy in asthma. *Pediatric Pulmonology,* pp. 27-31.

Hunt, Ward & King, 2013. Laser heating of sulfuric acid droplets held in air by Raman tweezers. *RSC Advances,* pp. 19448-19454.

Hunt, Ward & King, 2015. Heterogeneous oxidation of nitrite anion by gas phase ozone in an aqueous droplet levitated by laser tweezers (optical trap): is there any evidence for enhanced surface reaction?. *Physical Chemistry Chemical Physics,* pp. 2734-2741.

Icha, 2007. Ventolin remains a breath of fresh air for asthma sufferers, after 40 years. *The Pharmaceutical Journal,* p. 404.

Jones, King & Ward, 2015. Atmospherically relevant core-shell aerosol studied using optical trapping and Mie scattering. *Chemical Communications,* pp. 4914-4917.

Kwon, et al., 1994. Vibrational Spectroscopic Investigation of Benzoic Acid Adsorbed on Silver. *Journal of Physical Chemistry,* pp. 8481-8487.

Labiris & Dolovich, 2003. Pulmonary drug delivery. Part I: Physiological factors affecting therapeutic effectiveness of aerosolized medications. *Journal of Clinical Pharmacology,* p. 588–599.

Lavorini, et al., 2011. Retail sales of inhalation devices in European countries: So much for a global policy. *Respiratory Medicine,* pp. 1099-1103.

Lawrence, 2005. The relationship between relative humidity and the dew point temperature in moist air: A simple conversion and applications. *Bulletin of the American Meterorological Society,* pp. 225-233.

Leach, 2005. The CFC to HFA Transition and Its Impact on Pulmonary Drug Development. *Respiratory Care,* 50(9), pp. 1201-1208.

Lee, et al., 2012. The Efficacy of Immediate Diet for Reducing Local Adverse Events of Inhaled Corticosteroid: A Pilot Study. *Tuberculosis and Respiratory Diseases,* pp. 93-99.

Leger, Goursolle & Gadret, 1978. Structure Cristalline du Sulfate de Salbutamol [tert-Butylamino-2 (Hydroxy-4 hydromethyl-3 phenyl)-1 Ethanol.1/2H2SO4]. *Acta Crystallographica Section B,* pp. 1203-1208.

Lide, 1991. *CRC Handbook of Chemistry and Physics.* Boca Raton, FL: CRC Press.

Ling & Chan, 2008. Partial crystallization and deliquescence of particles containing ammonium sulfate and dicarboxylic acids. *Journal of Geophysical Research,* 113(14), pp. 1-15.

Lipasek, et al., 2013. Effect of Temperature on the Deliquescence Properties of Food Ingredients and Blends. *Journal of Agricultural and Food Chemistry,* pp. 9241-9250.

Lipworth & Jackson, 2000. Safety of Inhaled & Intranasal Corticosteroids Lessons for the New Millennium. *Drug Safety,* 1(23), pp. 11-33.

Macrae, et al., 2006. Mercury: visualization and analysis of crystal structures. *Journal of Applied Crystallography,* Volume 39, pp. 453-457.

Mutch, et al., 2007. The role of esterases in the metabolism of ciclesonide to desisobutyryl-ciclesonide in human tissue. *Biochemical Pharmacology,* pp. 1657-1664.

Nave, 2004. *Saturated Vapor Pressure, Density for Water.* [Online]
Available at: http://hyperphysics.phy-astr.gsu.edu/HBASE/Kinetic/watvap.html#c1
[Accessed 6th August 2014].

Pandya, Berawala, Khatri & Mehta, 2010. Spectrofluorimetric estimation of salbutamol sulphate in different dosage forms by formation of inclusion complex with β-cyclodextrin. *Pharmaceutical Methods,* pp. 49-53.

PerkinElmer Inc, 2008. *Advantages of Raman Spectroscopy when Analysing Materials through Glass or Polymer Containers and in Aqueous Solution.* [Online]
Available at:
http://www.perkinelmer.co.uk/CMSResources/Images/APP_RamanAnalysisTthrougGlassPolymerAqueous.pdf
[Accessed 07 August 2014].

Phull, Rao & Kankan, 2012. United States of America, Patent No. US 8158780 B2.

Purewal & Grant, 1997. *Metered Dose Inhaler Technology (Illustrated ed.).* s.l.:Informa Health Care.

Reisine, Heisler, Hook & Axelrod, 1983. Activation of beta 2-adrenergic receptors on mouse anterior pituitary tumor cells increases cyclic adenosine 3':5'-monophosphate synthesis and adrenocorticotropin release. *The Journal of Neuroscience,* pp. 725-732.

Renner, Mueller & Shephard, 2012. Environmental and non-infectious factors in the aetiology of pharyngitis (sore throat). *Inflammation Research,* pp. 1041-1052.

Rkiouak, et al., 2014. Optical trapping and Raman spectroscopy of solid particles. *Physical Chemistry Chemical Physics,* pp. 11426-11434.

Rogueda, et al., 2011. Particle synergy and aerosol performance in non-aqueous liquid of two combinations metered dose inhalation formulations: An AFM and Raman investigation. *Journal of Colloid and Interface Science,* pp. 649-655.

Sanders, 2007. Inhalation therapy: an historical review. *Primary Care Respiratory Journal,* pp. 71-81.

Sauer, Hofkens & Enderlein, 2011. *Handbook of Fluorescence Spectroscopy and Imaging.* Weinheim: WILEY-VCH Verlag GmbH.

Tang, et al., 2014. Heterogeneous interaction of SiO2 with N2O5: single particle optical levitation-Raman spectroscopy and aerosol flow tube studies. *The Journal of Physical Chemistry,* pp. 8817-8827.

Theophilus, et al., 2006. Co-deposition of salmeterol and fluticasone propionate by a combination inhaler. *International Journal of Pharmaceuticals,* pp. 14-22.

Tong, et al., 2014. Rapid interrogation of the physical and chemical characteristics of salbutamol sulphate aerosol from a pressurised metered-dose inhaler (pMDI). *Chemical Communications,* pp. 15499-15502.

Ullman & Svedmyr, 1988. Salmeterol, a new long acting inhaled beta 2 adrenoceptor agonist: comparison with salbutamol in adult asthmatic patients. *Thorax,* pp. 674-678.

UNEP, 1987. *The Montreal Protocol on substances that deplete the ozone layer.,* Nairobi: UNEP.

Vankeirsbilck, et al., 2002. Applications of Raman spectroscopy in pharmaceutical analysis. *TrAC Trends in Analytical Chemistry,* pp. 869-877.

Wang, et al., 2014. Low-frequency shift dispersive Raman spectroscopy for the analysis of respirable dosage forms. *International Journal of Pharmaceutics,* Issue 469, pp. 197-205.

Woolcock, Lundback, Ringdal & Jacques, 1996. Comparison of addition of salmeterol to inhaled steroids with doubling of the dose of inhaled steroids.. *American Journal of Respiratory and Critical Care Medicine,* pp. 1481-1488.

York & Hanna, 1994. United States of America, Patent No. US5795594 A.

Zhejiang NetSun Co., Ltd., 2010. *ChemNet.com - Global Chemical Network.* [Online] Available at: http://www.chemnet.com/cas/ [Accessed 21 09 2015].